

# Design and synthesis of a nucleobase functionalized peptide hydrogel: *in vitro* assessment of anti-inflammatory and wound healing effects

Sourav Bhowmik,<sup>a</sup> Budhadev Baral,<sup>b</sup> Tanmay Rit,<sup>a</sup> Hem Chandra Jha<sup>b</sup> and Apurba K. Das<sup>\*a</sup>

<sup>a</sup>Department of Chemistry, Indian Institute of Technology Indore, Indore 453552, India

<sup>b</sup>Department of Biosciences and Biomedical Engineering, Indian Institute of Technology Indore, Simrol, Khandwa Road, Indore 453552, India

\*E-mail: [apurba.das@iiti.ac.in](mailto:apurba.das@iiti.ac.in)

## Table of Contents

| Sl. No | Content  | Page no. |
|--------|--|----------|
| 1.     | Materials and methods and Experimental Sections  | S3-S6    |
| 2.     | The formation of the precipitate in presence of the phosphate buffer pH = 7.4 by <b>NP2</b> and <b>NP3</b> respectively. (Fig. S1)                                       | S7       |
| 3.     | Self-aggregation of the synthesized <b>NPs</b> at 0 ns, 50 ns and 100 ns. (Fig. S2)  | S7       |
| 4.     | DOSY NMR spectrum of 10 mM <b>NP1</b> in D <sub>2</sub> O at 298K. (Fig. S3)   | S8       |
| 5.     | DOSY NMR spectrum of 10 mM <b>NP2</b> in D <sub>2</sub> O at 298K. (Fig. S4)   | S8       |
| 6.     | DOSY NMR spectrum of 10 mM <b>NP3</b> in D <sub>2</sub> O at 298K. (Fig. S5)   | S9       |
| 7.     | Circular dichroism spectrum of the <b>NP1</b> hydrogel. (Fig. S6)  | S9       |
| 8.     | PXRD spectrum of (a) <b>NP1</b> hydrogel (b) the synthesized gelator precursor <b>NP1</b> . (Fig. S7)  | S10      |
| 9.     | Rheological experiments amplitude sweep experiment of the <b>NP1</b> hydrogel. (Fig. S8)   | S10      |
| 10.    | Live-dead cell imaging on the fibroblast McCoy cell by the newly developed <b>NP1</b> hydrogel. The scale bar in all the images is 20 $\mu$ m. (Fig. S9)                 | S11      |
| 11.    | HPLC chromatograms depicts the degradation of the <b>NP1</b> hydrogel in the presence of the proteolytic enzymes (a) $\alpha$ -chymotrypsin (b) proteinase-K. (Fig. S10) | S12      |
| 12.    | The (%) of the compound remained after the degradation by the proteolytic enzymes (a) $\alpha$ -chymotrypsin (b) proteinase-K. (Fig. S11)                                | S12      |
| 13.    | The antibacterial activity of the synthesized <b>NP1</b> hydrogel was investigated against (a) Gram-negative E. coli and (b) Gram-positive B. subtilis. (Fig. S12)       | S13      |
| 14.    | FE-SEM images of the (a) control (without <b>NP1</b> hydrogel) (b) in the presence of the <b>NP1</b> hydrogel. (Fig. S13)  | S13      |
| 15.    | Synthetic procedure<br>Characterization  | S14-S17  |
| 16.    | <sup>1</sup> H NMR, <sup>13</sup> C NMR and Mass Spectra of all synthesized compounds.   | S18-S28  |

## Materials and Methods

The used solvents and reagents were purchased from commercially available sources like Alfa Aesar, Sigma Aldrich, Merck and Spectrochem Pvt. Ltd. India. 2-Amino-6-chloropurine and potassium carbonate ( $K_2CO_3$ ) were obtained from Alfa Aesar. Ethyl chloroformate was purchased from Spectrochem whereas diethyl ether was purchased from Merck. 4-Methylmorpholine was obtained from SRL and 6-bromohexanoic acid were obtained from TCI. L-Phenylalanine, L-tyrosine were purchased from SRL. Fetal bovine serum, MTT (3-(4,5-dimethyl-2-thiazolyl)-2,5-diphenyl-2H-tetrazolium bromide, Dulbecco's Modified Eagle Medium (DMEM) and Streptomycin were obtained from Himedia. FDA, DCFDA and propidium iodide were obtained from Invitrogen. For moisture sensitive reactions, dry solvent was used in the presence of  $N_2$  or Ar gas. After completion of the reaction, the crude products were purified by column chromatography method using silica as stationary phase and hexane, ethyl acetate or chloroform, methanol as a mobile phase. All  $^1H$  and  $^{13}C$  NMR spectra were set down on Bruker Avance (500 MHz) instrument at 25 °C. Mass spectra were set down on Bruker instrument by using ESI positive mode. The NMR spectra of all intermediates and final products were analyzed by using MestReNova software. Chemical shift was expressed in the form of ppm ( $\delta$ ) relative to surplus solvents protons as internal standards (DMSO- $d_6$ :  $\delta = 2.50$  for  $^1H$  NMR; DMSO- $d_6$ :  $\delta 39.50$  for  $^{13}C$  NMR).

## Molecular Dynamics (MD) Simulation

MD simulation was performed using Amber22. Geometry optimization was carried out before the simulation. AMBERff14SB force field was utilized to apply atom types. AM1-BCC charge set was used. Packmol was used to build the initial system of the simulation. The systems were built 120 molecules. These molecules were arranged randomly in the simulation box. TIP3P water model was used. General amber force field (GAFF) was used to take care any missing parameters. Periodic boundary conditions were implemented in each run. Berendsen barostat and Langevin thermostat maintained the constant pressure and temperature. The computational studies were carried using the following conditions. Initially two minimizations were carried out with 1000 cycles of steepest descent algorithm and 500 cycles of conjugate gradient algorithm. The temperature of the system was increased to 300K. Then, equilibration was carried out. The Final simulation runs were performed upto 100 ns. The solvent accessible surface area was analyzed by CPPTRAJ.

## Experimental Sections

**HPLC Analysis:** The progress of biocatalyst driven reactions was monitored using a Dionex reverse-phase HPLC system, which was connected with a photodiode array detector (Ultimate 3000). A volume of 30 microliters of the sample was injected into a C-18 column with dimensions of  $4.6 \times 250$  mm, which contained fused silica particles measuring 5 micrometres in diameter. The injection was performed at a flow rate of 1 mL per minute. The material was eluted using a gradient of water (A) and acetonitrile (B) over a period of 42 minutes (0-4 min %A: 80, %B: 20; 4-35 min %A: 20, %B: 80; 35-40 min %A: 20, %B: 80, 40-42 min %A: 80, %B: 20). The preparation of the sample included dissolving the necessary amount of peptide in a 1 mL solution of acetonitrile and water in a 1:1 ratio.

**CD Spectroscopy:** A Jasco J-1500 CD spectrophotometer (Easton, MD, USA) was used to quantify the CD of each peptide hydrogel. CD spectra were recorded with quartz cuvette with a 0.1 mm path length and a maximum chamber capacity of 800  $\mu$ L. Spectra for of the **NP1** hydrogel was acquired in the 190–300 nm region. The programme JASCO spectra manager was used to analyze the acquired spectra.

**FTIR Spectroscopy:** The hydrogel was dried by lyophilizer to obtained powder. ATR-FTIR spectra of the dried hydrogel and the corresponding gelator precursor was acquired using bruker make Vertex 70 instrument. The spectra were recorded from  $400\text{ cm}^{-1}$  to  $4000\text{ cm}^{-1}$  at a resolution of  $2\text{ cm}^{-1}$ , and the data was processed using OPUS 6.5 software. We used background subtraction to get rid of the atmospheric interference.

**ThT Dye Binding Assay:** The method used to conduct the ThT binding test was the same as that which was disclosed in our prior research. The resulting NP1 hydrogel was diluted and exposed to a 0.5 mM thioflavin-T solution for 15 minutes. To investigate the existence of secondary structures in the co-assembled gels, the samples were stimulated at a wavelength of 450 nm, and the emission spectra were recorded using Horiba spectrometer.

**Rheological Experiment:** The hydrogels' mechanical rigidity was achieved by using a method similar to that reported in our previous studies. Just before measurement, the hydrogels were quickly demolded in the bottom plate of the rheometer. An Anton Parr MCR301 rheometer was used to measure the mechanical properties of the hydrogels using a parallel plate geometry with a

25 mm diameter (PP25). For the sake of repeatability, the measurements were carried out three times, and the average result is shown.

### **Morphological Investigation**

**Scanning Electron Microscopy:** Microscopic methods were used to characterize self-assembled nano structural morphology in the synthesized **NP1** hydrogel. The nano structural morphology inside the hydrogel was visualized by Field-emission scanning electron microscope (FE-SEM model Zeiss Supra55). The **NP1** hydrogel was diluted before taking images. 50  $\mu\text{L}$  of **NP1** hydrogel (20 mM) was diluted with 150  $\mu\text{L}$  of the deionized water. 20  $\mu\text{L}$  of the diluted hydrogel solution was placed on a glass slide. The **NP1** hydrogel on a glass slide was dried twice: once in the air and once under vacuum before being gold-coated.

**Transmission Electron Microscopy:** Transmission electron microscopy images (TEM) were taken using a field-emission gun TEM (model: Tecnai G2, F30). TEM was operated at a voltage of 200 kV. The **NP1** hydrogel was dilute before taking images. The diluted solution of the **NP1** hydrogel was placed on carbon-coated copper grids. The mesh size of the copper grid was 300. Hydrogel solution on the copper grid was dried at room temperature. **NP1** hydrogel (50  $\mu\text{L}$ ) was dissolved in 450  $\mu\text{L}$  of water. TEM investigations were used to examine the nanostructural shape of hydrogels using 3% phosphotungstic acid as a negative stain.

**Wound Healing Assay:** The cells were seeded into a 6-well plate and continuously cultured to reach the confluency level of 100% to form a monolayer. A single line wound was formed by scratching the cell through a 1000  $\mu\text{l}$  pipette tip and then washed with PBS. Then, the cells were treated with hydrogel. Only PBS was used as control. Thereafter, images were captured through a light microscope (DM21, Leica microsystems, Germany) after an incubation period of 0, 12, 24, 36 and 48 h, and then the wound area was quantified using ImageJ software.

### **Antibacterial Experiment**

**Bacterial Culture:** The microorganisms *Bacillus subtilis* (MTCC 619) and *Escherichia coli* (MTCC 739) were purchased from the Institute of Microbial Technology Chandigarh, India, as a lyophilized powder. Fresh inoculums of the Gram-positive bacteria *B. subtilis* as well as the Gram-negative bacteria *E. coli* were made prior to the tests. A single colony was taken out and afterwards injected into nutrient broth medium that had been autoclaved to promote bacterial growth.

Overnight, the bacterial inoculums were incubated at 37 °C in an incubator. Fresh overnight bacterial suspensions were diluted to a workable concentration of  $1-2 \times 10^8$  colony-forming units (cfu mL<sup>-1</sup>) by diluting them with 0.5 McFarland standards. All cultures had their optical densities evaluated at 625 nm under aseptic circumstances both before and after incubation. Reading was taken using Mutiskan FC plate reader.

**Culture Media:** The liquid medium used for bacterial culture was called nutrient broth medium, and it was made by combining peptone (10 g), yeast extracts (3 g), and sodium chloride (5 g, NaCl) with 1000 mL of sterile distilled water. Agar-agar powder (15 g) was added to 1000 mL of nutrient broth medium to create the nutrient agar medium. Using NaOH (0.1 N) solution, the pH of the nutrient broth and nutrient agar media was brought to 7.0. In a 25 mL Erlenmeyer flask, the nutrient broth and nutrient agar media were sterilised for 30 minutes at 121 °C and 15 lbs of pressure.

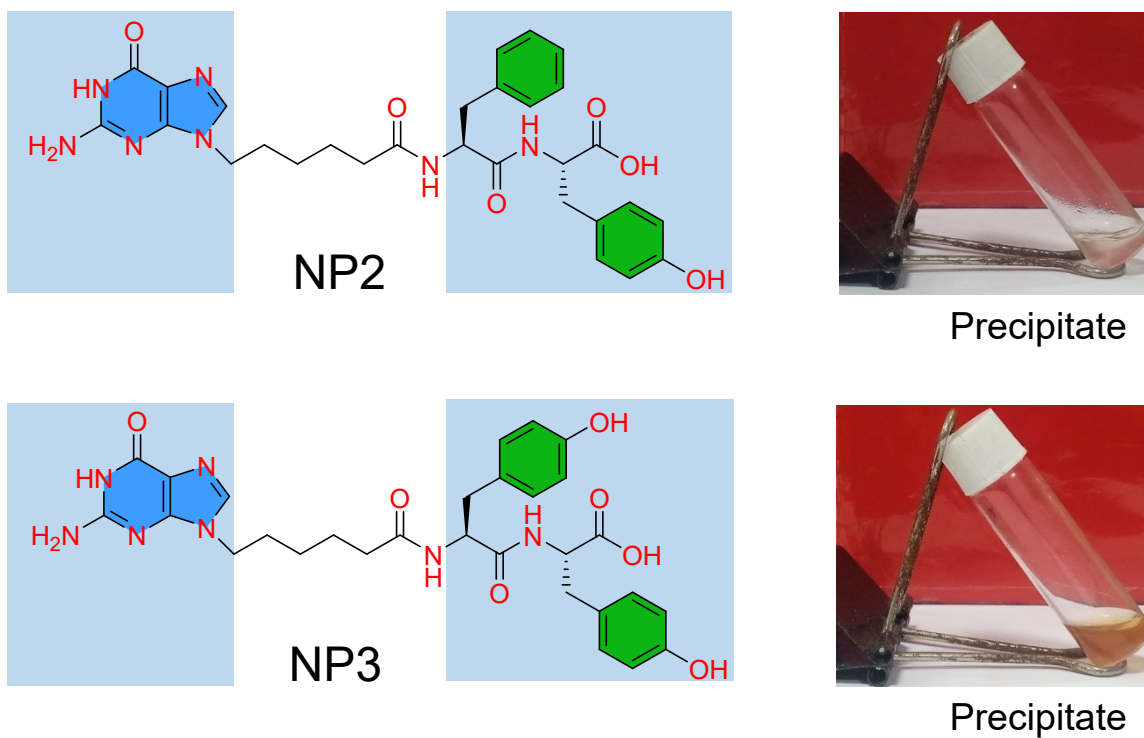


**Fig. S1** The formation of the precipitate in presence of the phosphate buffer pH = 7.4 by NP2 and NP3 respectively.

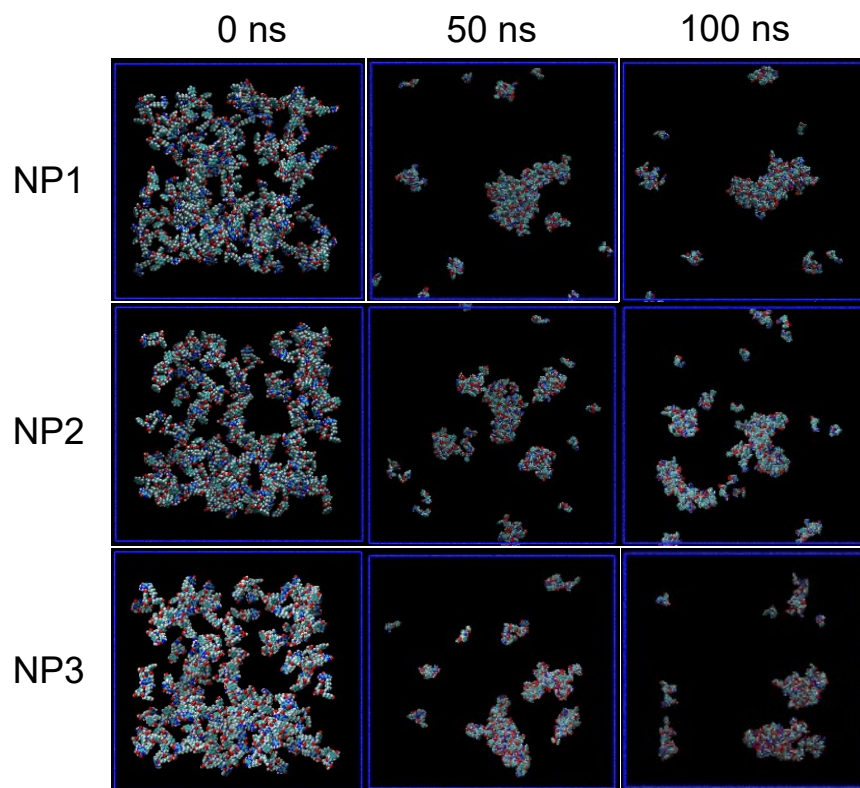


**Fig. S2** Self-aggregation of the synthesized NPs at 0 ns, 50 ns and 100 ns.

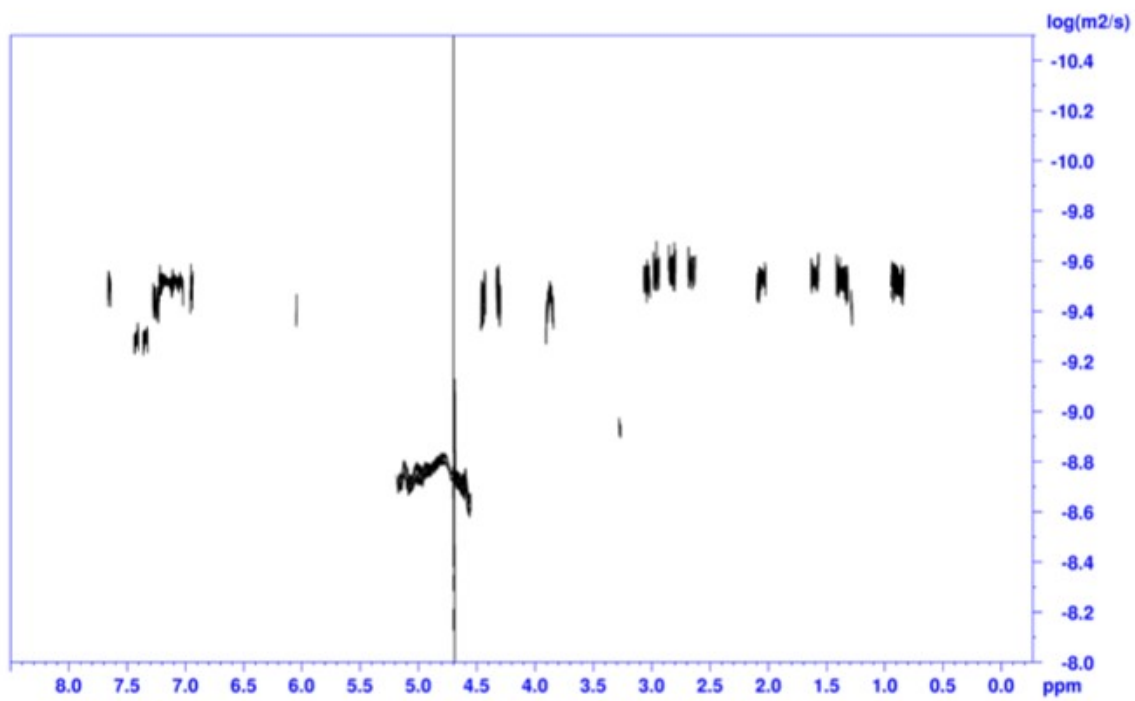


**Fig. S3** DOSY NMR spectrum of 10 mM NP1 in D<sub>2</sub>O at 298K.

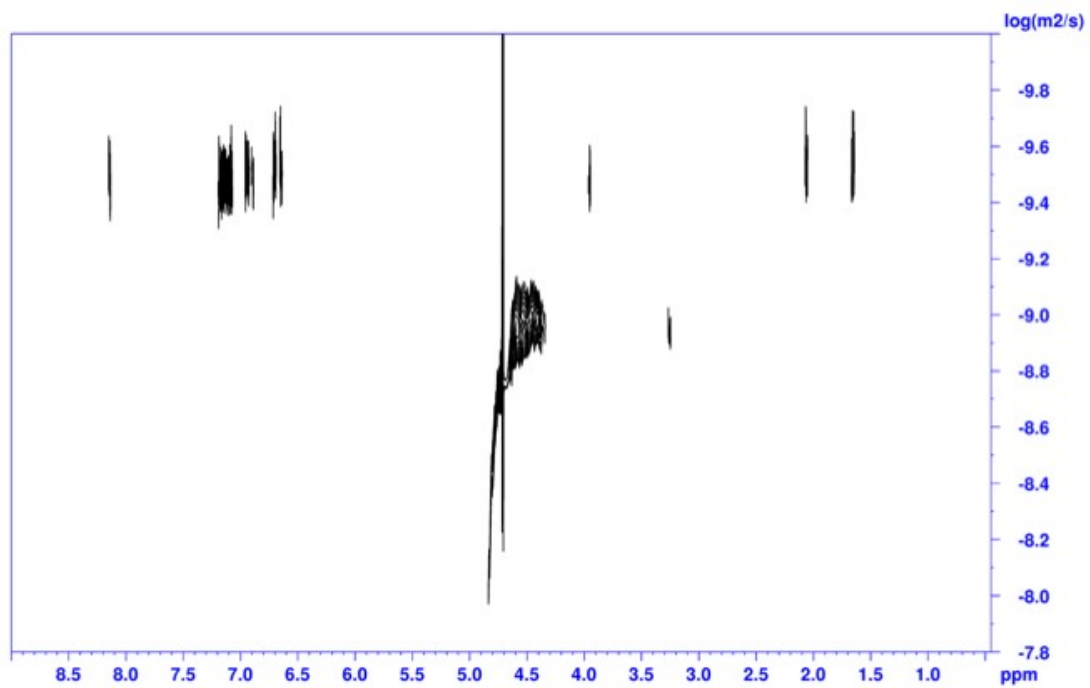


**Fig. S4** DOSY NMR spectrum of 10 mM NP2 in D<sub>2</sub>O at 298K.

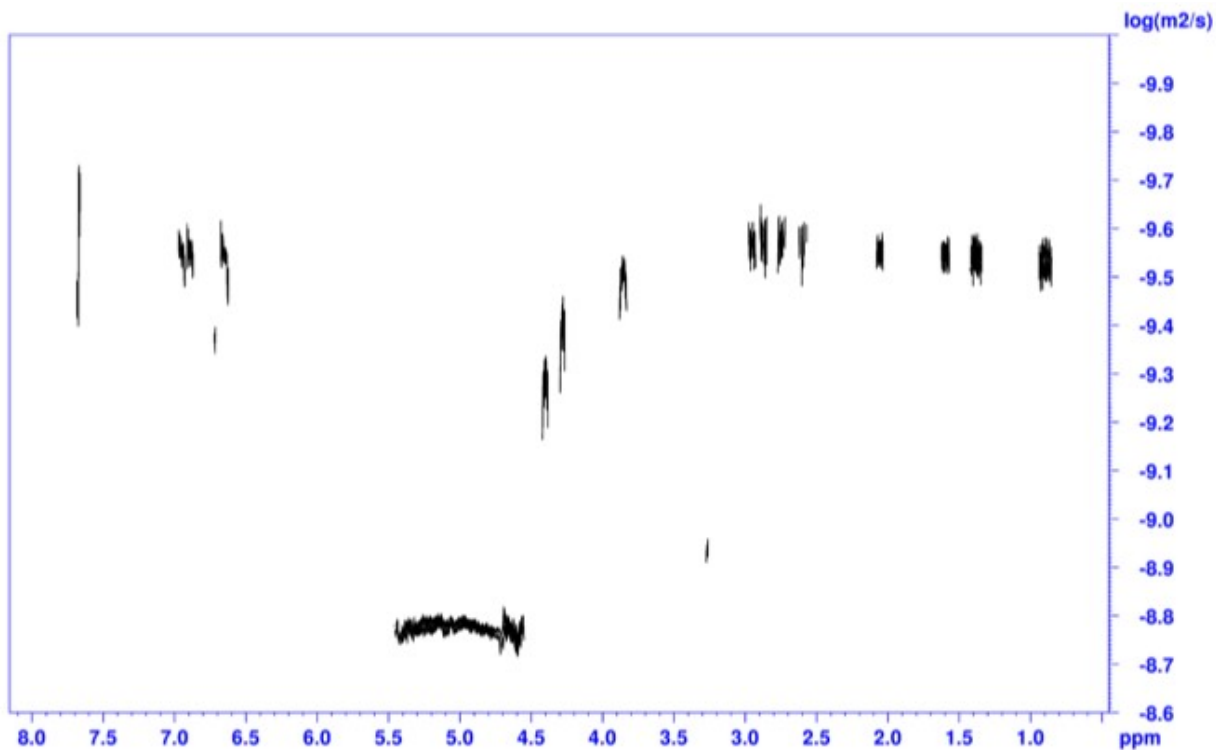


**Fig. S5** DOSY NMR spectrum of 10 mM **NP3** in D<sub>2</sub>O at 298K

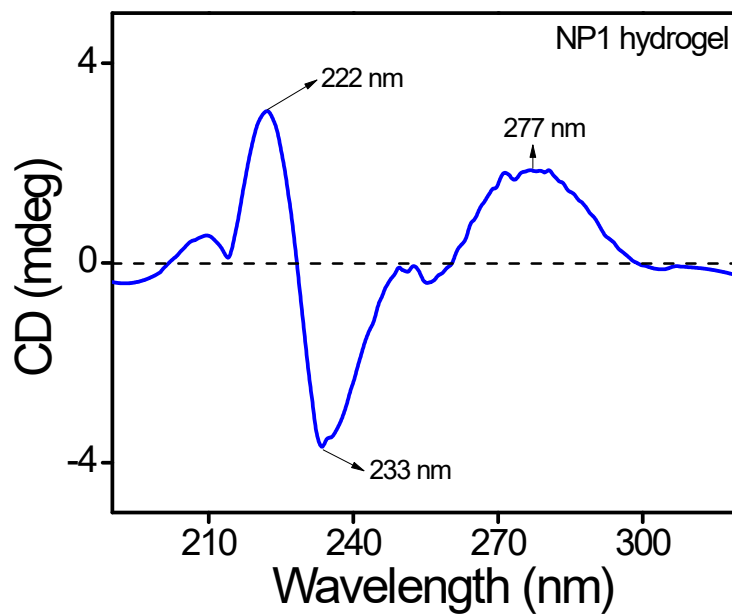


**Fig. S6** Circular dichroism spectrum of the **NP1** hydrogel.

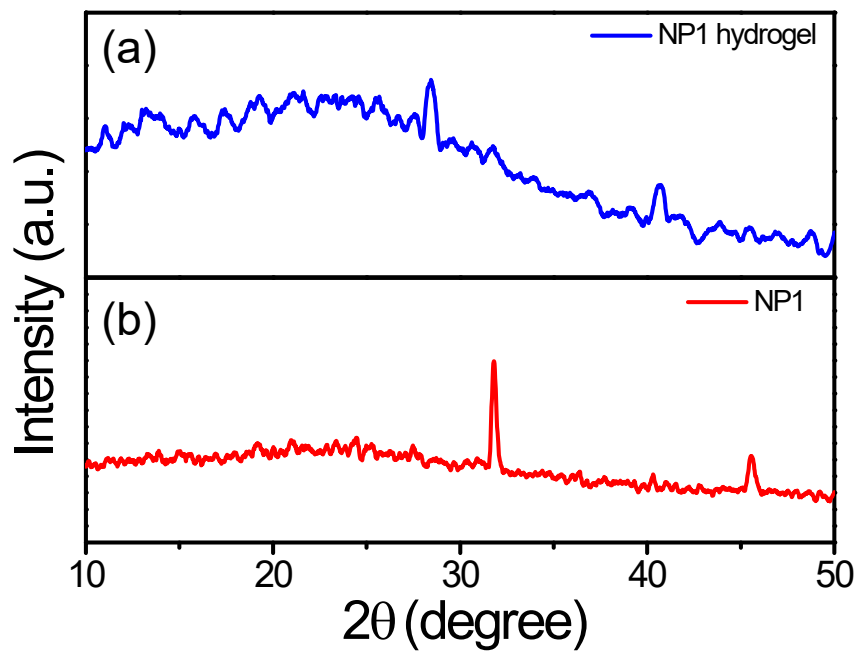


**Fig. S7** PXR D spectrum of (a) NP1 hydrogel (b) the synthesized gelator precursor NP1.

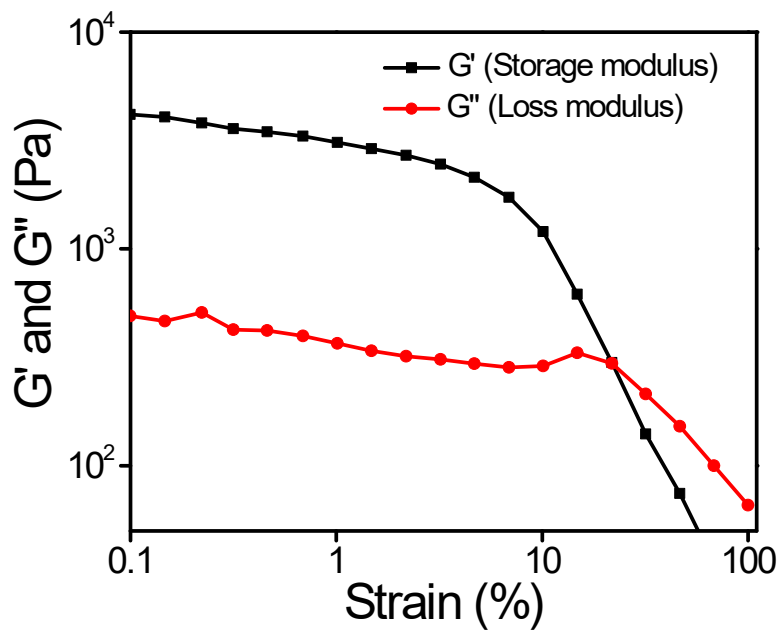


**Fig. S8** Amplitude sweep experiment of the NP1 hydrogel.

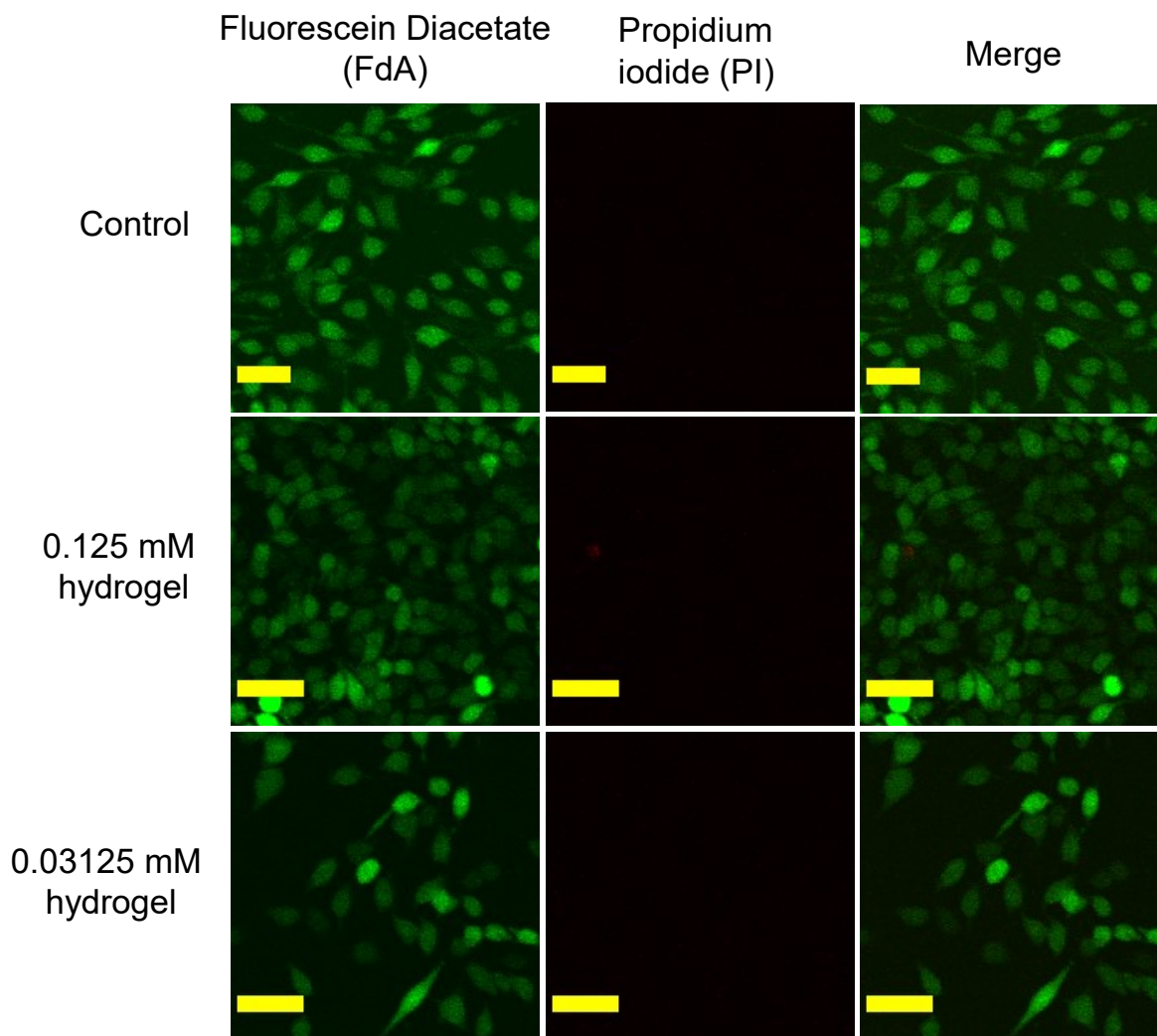


**Fig. S9** Live-dead cell imaging on the fibroblast McCoy cell by the newly developed NP1 hydrogel. The scale bar in all the images is 20  $\mu\text{m}$ .

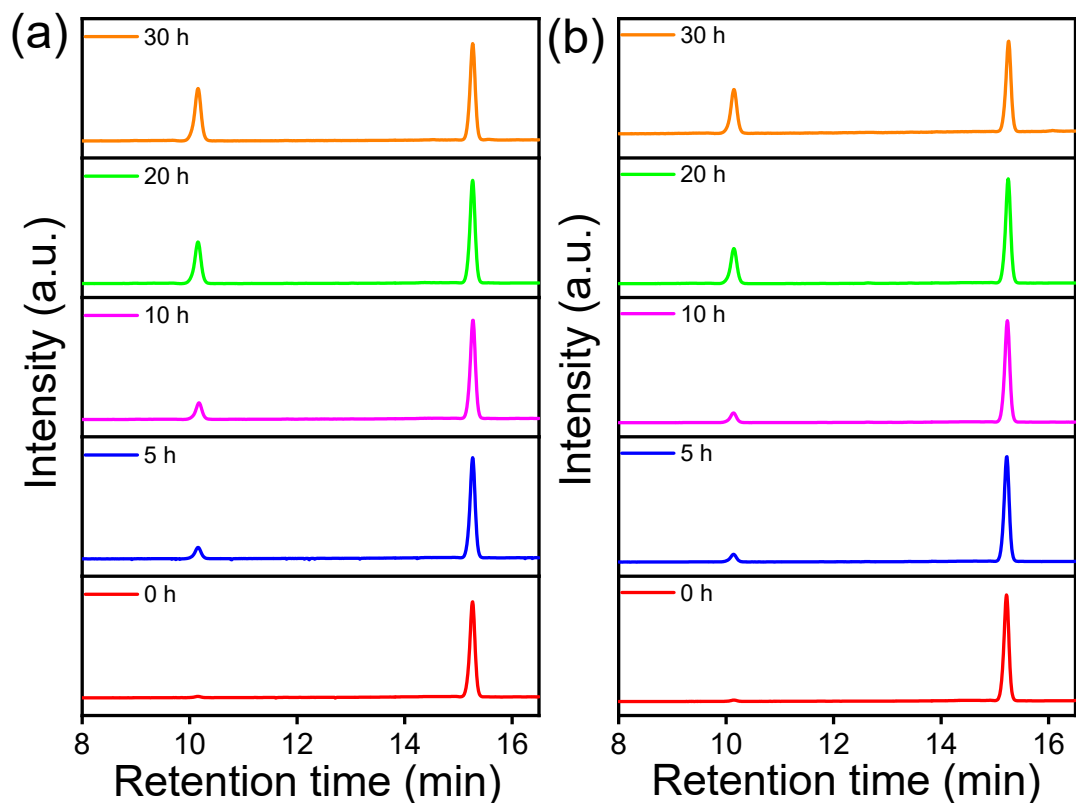


**Fig. S10** HPLC chromatograms depicts the degradation of the NP1 hydrogel in the presence of the proteolytic enzymes (a)  $\alpha$ -chymotrypsin (b) proteinase-K.

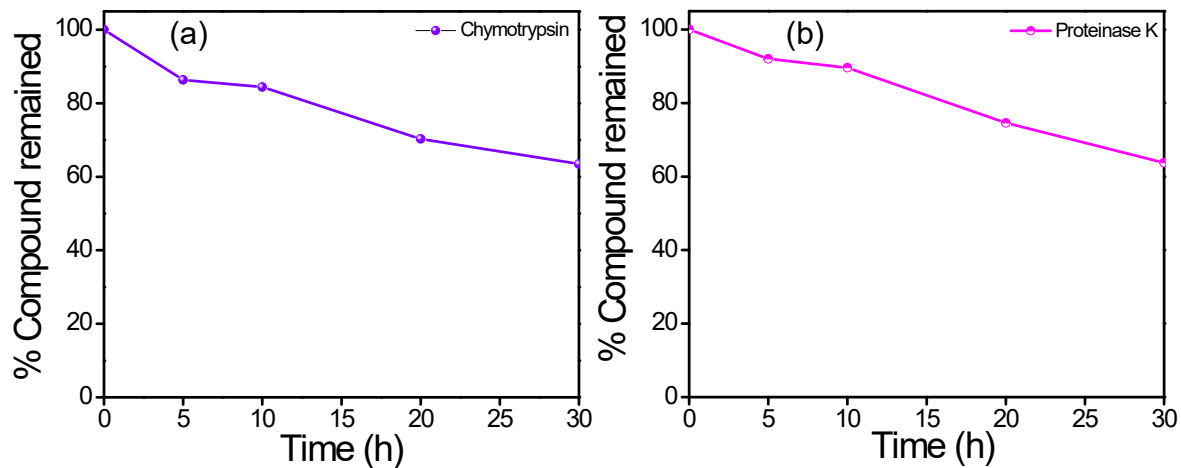


**Fig. S11** The (%) of the compound remained after the degradation by the proteolytic enzymes (a)  $\alpha$ -chymotrypsin (b) proteinase-K.

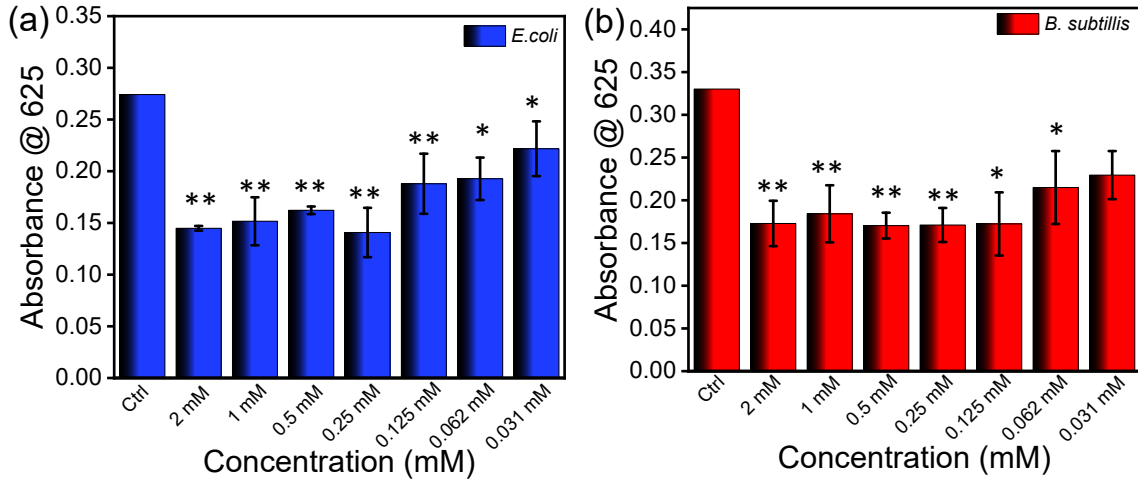


**Fig. S12** The antibacterial activity of the synthesized NP1 hydrogel was investigated against (a) Gram-negative *E. coli* (b) Gram-positive *B. subtilis*. All the results were derived from technical triplicate ( $N = 3$ ). All the data were statistically analyzed by unpaired  $t$ -test using graphpad prism trial version. \* $p < 0.05$ , \*\* $p < 0.01$  as compared to the control.

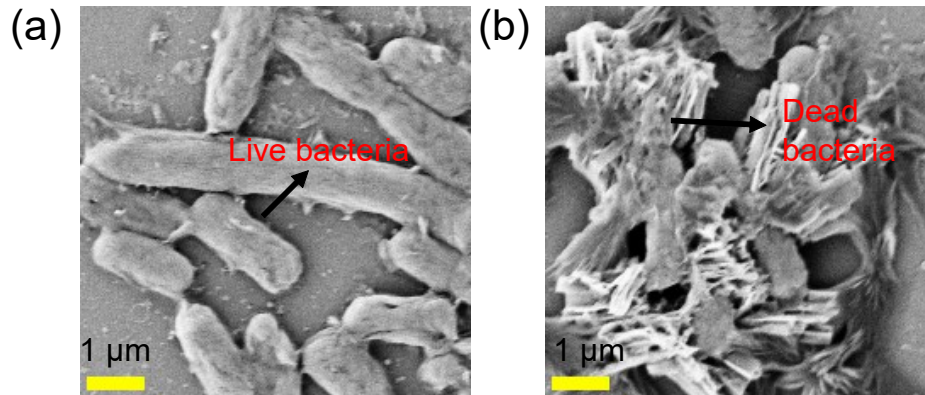
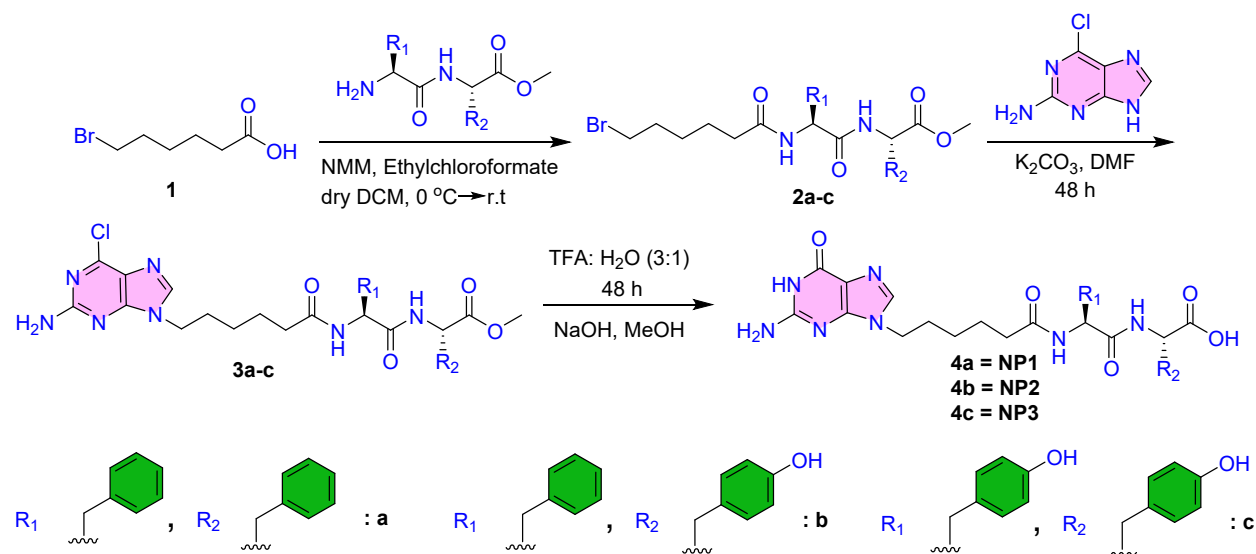


**Fig. S13** FE-SEM images of the *E. coli* bacteria (a) control (without NP1 hydrogel) (b) in the presence of the NP1 hydrogel.

## Synthetic Scheme:



### General procedure for the synthesis of **2a-c**:

Under argon atmosphere 4-methylmorpholine was added in the solution of 6-bromohexanoic acid in dry chloroform at 0 °C. The solution was left for stirring at this temperature. After 15 min, ethyl chloroformate was added into the solution and stirred vigorously at this temperature for additional 45 min before the addition of acid protected dipeptide and 4-methylmorpholine. Then the reaction mixture was allowed to stir for 1 h at 0 °C and then at room temperature for 16 h. The progress of the reaction was monitored by TLC. After the completion of the reaction, reaction mixture was diluted with chloroform and washed with 1(N) NaOH (3×10 mL) and then with brine, 1 (N) HCl (3×10 mL) and finally with brine. The organic part was dried over Na<sub>2</sub>SO<sub>4</sub> and concentrate under vacuum.

### Synthesis of **2a**:

Yield: 94% <sup>1</sup>H NMR (DMSO-*d*<sub>6</sub>, 400 MHz): 1.19-1.28 (m, 2H), 1.35-1.46 (m, 2H), 1.72-1.79 (m, 2H), 2.04-2.07 (t, 2H, *J* = 4, 8 Hz), 2.71-2.77 (m, 1H), 2.99-3.04 (m, 1H), 3.08-3.13 (m, 1H), 3.48-3.51 (t, 2H, *J* = 4, 8 Hz), 3.65 (s, 1H), 4.53-4.58 (m, 1H), 4.60-4.65 (m, 1H), 7.24-7.36 (m, 10H), 8.02-8.04 (d, 1H, *J* = 4 Hz), 8.47-8.49 (d, 1H, *J* = 4 Hz). (ESI-MS, *m/z*): [M+Na]<sup>+</sup> calculated for C<sub>25</sub>H<sub>31</sub>BrN<sub>2</sub>O<sub>4</sub>Na 525.1359; found 525.1152

### Synthesis of **2b**:

Yield: 90%. <sup>1</sup>H NMR (DMSO-*d*<sub>6</sub>, 500 MHz): 1.14-1.20 (m, 2H), 1.31-1.40 (m, 2H), 1.58-1.73 (m, 2H), 2.66-2.71 (m, 1H), 2.82-2.99 (m, 4H), 3.43-3.45 (t, 1H, *J* = 5, 5 Hz), 3.53-3.55 (t, 1H, *J* = 5, 5 Hz) 3.58 (s, 3H), 4.38-4.43 (m, 1H), 4.55-4.60 (m, 1H), 6.65-6.67 (d, 2H, *J* = 10 Hz), 6.99-7.00 (d, 2H, *J* = 5 Hz), 7.16-7.27 (m, 5H) 7.97-7.99 (d, 1H, *J* = 10 Hz), 8.33-8.34 (d, 1H, *J* = 5 Hz), 9.23 (s, 1H). (ESI-MS, *m/z*): [M+Na]<sup>+</sup> calculated for C<sub>25</sub>H<sub>31</sub>BrN<sub>2</sub>O<sub>5</sub>Na 541.1416; found 541.1010.

#### Synthesis of **2c**:

Yield: 92%. <sup>1</sup>H NMR (DMSO-*d*<sub>6</sub>, 400 MHz): 1.19-1.24 (m, 2H), 1.36-1.39 (m, 2H), 1.61-1.75 (m, 2H), 1.99-2.03 (t, H, *J* = 8, 8 Hz), 2.80-2.93 (m, 4H), 3.44-3.47 (t, 2H, *J* = 4, 8 Hz), 3.57 (s, 1H), 4.36-4.41 (m, 1H), 4.44-4.47 (m, 1H), 6.62-6.66 (t, 4H, *J* = 8, 8 Hz), 6.97-7.02 (t, 4H, *J* = 8, 12 Hz), 7.88-7.90 (d, 1H, *J* = 8 Hz) 8.26-8.28 (d, 1H, *J* = 8 Hz), 9.13 (s, 1H), 9.22 (s, 1H). (ESI-MS, *m/z*): [M+Na]<sup>+</sup> calculated for C<sub>25</sub>H<sub>31</sub>BrN<sub>2</sub>O<sub>6</sub>Na 557.1365; found 557.1105.

#### General procedure for the synthesis of **3a-c**:

Here, the compounds were synthesized following previously reported synthetic procedure. 2-Amino-6-chloropurine was added in the solution of dry DMF (10 mL) under argon atmosphere. Then K<sub>2</sub>CO<sub>3</sub> was added in the solution. Finally, 6-bromohexanoic acid was added dropwise into the solution and the reaction was left for stirring for 24 h. The progress of the reaction was monitored by TLC. After the completion of the reaction, the reaction mixture was diluted with ethyl acetate and washed with water several times, finally with brine and dried over Na<sub>2</sub>SO<sub>4</sub>. After the evaporation of the solvent under rotary evaporator, the reaction mixture was purified by silica gel column chromatography. The major product was N9 alkylated product (eluent: CHCl<sub>3</sub>: MeOH = 99:1) and the minor product was N7 alkylated product (eluent: CHCl<sub>3</sub>: MeOH = 94:6).

#### Synthesis of **3a**:

Yield: 74%. <sup>1</sup>H NMR (DMSO-*d*<sub>6</sub>, 500 MHz): 1.01-1.07 (m, 2H), 1.36-1.40 (m, 2H), 1.62-1.70 (m, 2H), 1.97-2.00 (t, 2H, *J* = 5, 10 Hz), 2.64-2.69 (m, 2H), 2.93-2.98 (m, 2H), 3.02-3.06 (m, 1H), 3.58 (s, 3H), 3.93-3.96 (t, 2H, *J* = 5, 10 Hz), 4.47-4.51 (m, 1H), 4.53-4.58 (m, 1H), 6.90 (s, 2H), 7.14-7.29 (m, 5H) 7.94-7.96 (d, 1H, *J* = 10 Hz), 8.10 (s, 1H), 8.42-8.44 (d, 1H, *J* = 10 Hz), 9.23 (s, 1H). (ESI-MS, *m/z*): [M+Na]<sup>+</sup> calculated for C<sub>30</sub>H<sub>34</sub>ClN<sub>7</sub>O<sub>4</sub>Na 614.2361; found 614.2266.

#### Synthesis of **3b**:

Yield: 70%. <sup>1</sup>H NMR (DMSO-*d*<sub>6</sub>, 500 MHz): 0.99-1.05 (m, 2H), 1.32-1.40 (m, 2H), 1.62-1.68 (m, 2H), 1.96-1.99 (d, 2H, *J* = 5, 10 Hz), 2.62-2.67 (m, 1H), 2.79-2.84 (m, 1H), 2.87-2.96 (m, 2H), 3.56 (s, 1H), 3.92-3.94 (t, 1H, *J* = 5, 10 Hz), 4.36-4.40 (m, 1H), 4.51-4.56 (m, 1H), 6.63-6.64 (d, 2H, *J* = 5 Hz), 6.87 (s, 2H), 6.97-6.98 (d, 2H, *J* = 5 Hz), 7.12-7.21 (m, 5H), 7.93-7.95 (d, 2H, *J* = 10 Hz) 8.07 (s, 1H), 8.32-8.33 (d, 1H, *J* = 5 Hz), 9.27 (s, 1H). (ESI-MS, *m/z*): [M+H]<sup>+</sup> calculated for C<sub>30</sub>H<sub>35</sub>CIN<sub>7</sub>O<sub>5</sub> 608.2310; found 608.2286.

#### Synthesis of **3c**:

Yield: 72%. <sup>1</sup>H NMR (DMSO-*d*<sub>6</sub>, 500 MHz): 1.04-1.11 (m, 2H), 1.36-1.42 (m, 2H), 1.66-1.71 (m, 2H), 1.99-2.02 (d, 2H, *J* = 5, 10 Hz), 2.81-2.92 (m, 4H), 3.57 (s, 3H), 3.94-3.97 (t, 1H, *J* = 5, 10 Hz), 4.37-4.41 (m, 1H), 4.45-4.49 (m, 1H), 6.62-6.66 (m, 4H), 6.91 (s, 2H), 6.98-7.02 (m, 4H), 7.88-7.89 (d, 2H, *J* = 5 Hz), 8.10 (s, 1H), 8.29-8.30 (d, 1H, *J* = 5 Hz), 9.15 (s, 1H), 9.23 (s, 1H). (ESI-MS, *m/z*): [M+H]<sup>+</sup> calculated for C<sub>30</sub>H<sub>35</sub>CIN<sub>7</sub>O<sub>6</sub> 624.2259; found 624.2375.

#### General procedure for the synthesis of compound **NP1-3**:

These compounds were synthesized based on the previously reported synthetic procedure. These compounds were dissolved in the TFA: H<sub>2</sub>O (3:1) 5 mL. Then, the reaction was left for stirring for a period of 48 h at room temperature. The progress of the reaction was monitored by HPLC. After the completion of the oxidation reaction, TFA was evaporated under vacuum. Then the residue was dissolved in MeOH, dropwise 1(N) NaOH was added to get the completely hydrolyzed product. The progress of the hydrolysis was also monitored by HPLC. After the completion of the hydrolysis, MeOH was evaporated under vacuum, and then it was dissolved in water, and also washed with diethyl ether. Then, after washing the pH of the solution was slowly decreased to obtain the white precipitate. Then it was recrystallized in MeOH to obtain the pure product.

#### Synthesis of **NP1**:

Yield: 88%. <sup>1</sup>H NMR (DMSO-*d*<sub>6</sub>, 500 MHz): 0.93-1.00 (m, 2H), 1.26-1.32 (m, 2H), 1.51-1.59 (m, 2H), 1.89-1.96 (m, 2H), 2.54-2.63 (m, 1H), 2.83-2.93 (m, 2H), 3.00-3.03 (m, 1H), 3.74-3.77 (t, 2H, *J* = 5, 10 Hz), , 4.30-4.35 (m, 1H), 4.40-4.46 (m, 1H), 6.45 (s, 1H), 7.09-7.20 (m, 10H), 7.57 (s, 1H), 7.92-7.93 (d, 1H, *J* = 5 Hz) 8.04-8.05 (d, 1H, *J* = 5 Hz), 10.57 (s, 1H). <sup>13</sup>C NMR (DMSO-*d*<sub>6</sub>, 125 MHz): δ 25.06, 25.84, 29.64, 35.42, 37.35, 37.82, 42.91, 54.58, 54.84, 116.97, 126.48,

128.41, 129.93, 137.76, 138.73, 151.54, 154.32, 157.41, 171.32, 172.34, 173.39. (ESI-MS,  $m/z$ ):  $[M+Na]^+$  calculated for  $C_{29}H_{33}N_7O_5Na$  582.2435; found 582.2407.

#### Synthesis of **NP2**:

Yield: 85%.  $^1H$  NMR (DMSO- $d_6$ , 500 MHz): 0.98-1.07 (m, 2H), 1.32-1.38 (m, 2H), 1.58-1.64 (m, 2H), 1.97-2.00 (m, 2H), 2.65-2.70 (m, 1H), 2.80-2.84 (m, 1H), 2.93-3.01 (m, 2H), 3.81-3.84 (t, 1H,  $J = 5, 10$  Hz), 4.34-4.38 (m, 1H), 4.52-4.57 (m, 1H), 6.47 (s, 2H), 6.65-6.66 (d, 2H,  $J = 5$  Hz), 7.01-7.02 (d, 2H,  $J = 5$  Hz), 7.15-7.23 (m, 5H) 7.68 (s, 1H) 7.95-7.97 (d, 1H,  $J = 10$  Hz), 8.13-8.14 (d, 1H,  $J = 5$  Hz), 9.23 (s, 1H), 10.56 (s, 1H) 12.70 (s, 1H).  $^{13}C$  NMR (DMSO- $d_6$ , 125 MHz):  $\delta$  25.05, 25.84, 29.62, 35.39, 36.34, 37.92, 42.99, 53.86, 54.24, 115.45, 116.82, 126.62, 127.79, 128.39, 129.64, 130.55, 137.83, 138.46, 151.52, 153.98, 156.42, 157.20, 171.92, 172.25, 173.32. (ESI-MS,  $m/z$ ):  $[M+Na]^+$  calculated for  $C_{29}H_{33}N_7O_6Na$  598.2385; found 598.2380.

#### Synthesis of **NP3**:

Yield: 87%.  $^1H$  NMR (DMSO- $d_6$ , 500 MHz): 1.03-1.10 (m, 2H), 1.36-1.39 (m, 2H), 1.59-1.63 (m, 2H), 1.98-2.01 (m, 2H), 2.81-2.98 (m, 4H), 3.82-3.84 (t, 2H,  $J = 5, 5$  Hz), 4.19-4.21 (m, 1H), 4.35-4.38 (m, 1H), 6.61-6.64 (m, 4H), 6.66 (s, 2H), 6.96-7.02 (m, 4H), 7.64 (s, 1H) 7.80-7.81 (d, 1H,  $J = 5$  Hz), 7.98-8.00 (d, 1H,  $J = 10$  Hz), 9.21 (s, 2H), 10.89 (s, 1H).  $^{13}C$  NMR (DMSO- $d_6$ , 125 MHz):  $\delta$  25.12, 25.93, 29.76, 35.47, 36.42, 37.10, 42.98, 54.83, 54.85, 115.24, 117.00, 130.48, 130.73, 137.82, 151.55, 154.16, 156.14, 156.21, 157.42, 171.53, 172.32, 173.56. (ESI-MS,  $m/z$ ):  $[M+H]^+$  calculated for  $C_{29}H_{34}N_7O_7$  592.2514; found 592.2536.

## NMR and Mass spectra

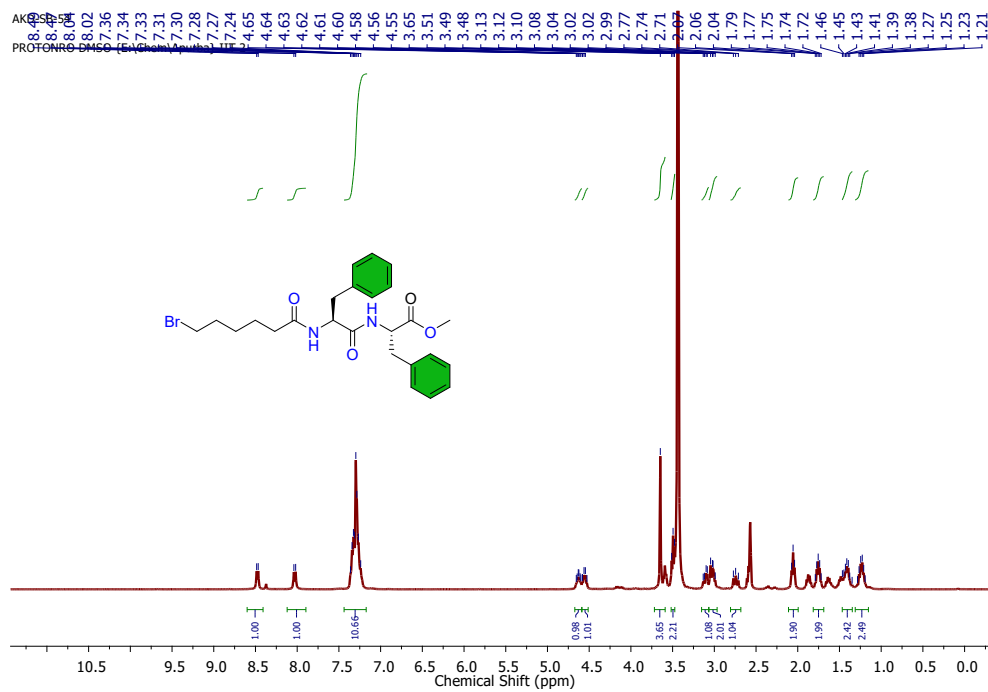


Fig. S14  $^1\text{H}$  NMR (500 MHz,  $\text{DMSO-}d_6$ ) spectrum of **2a**.

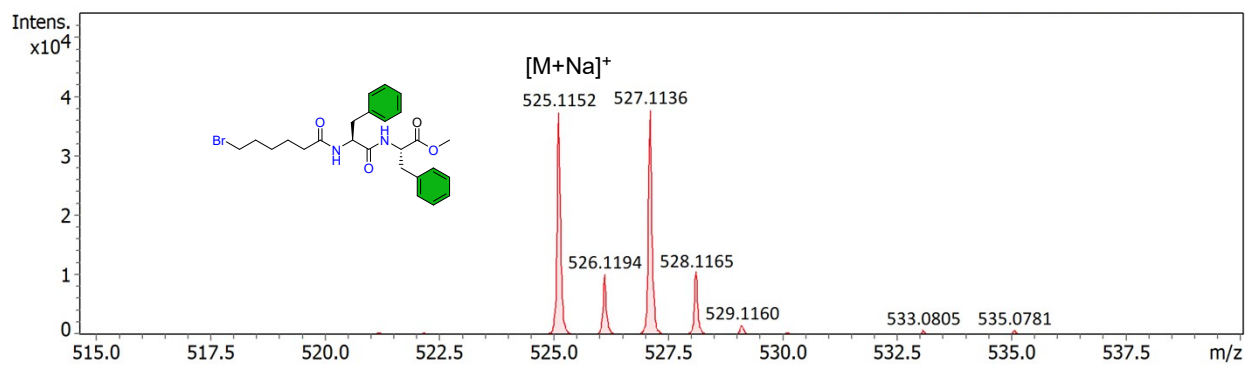


Fig. S15 ESI-MS spectrum of **2a**.

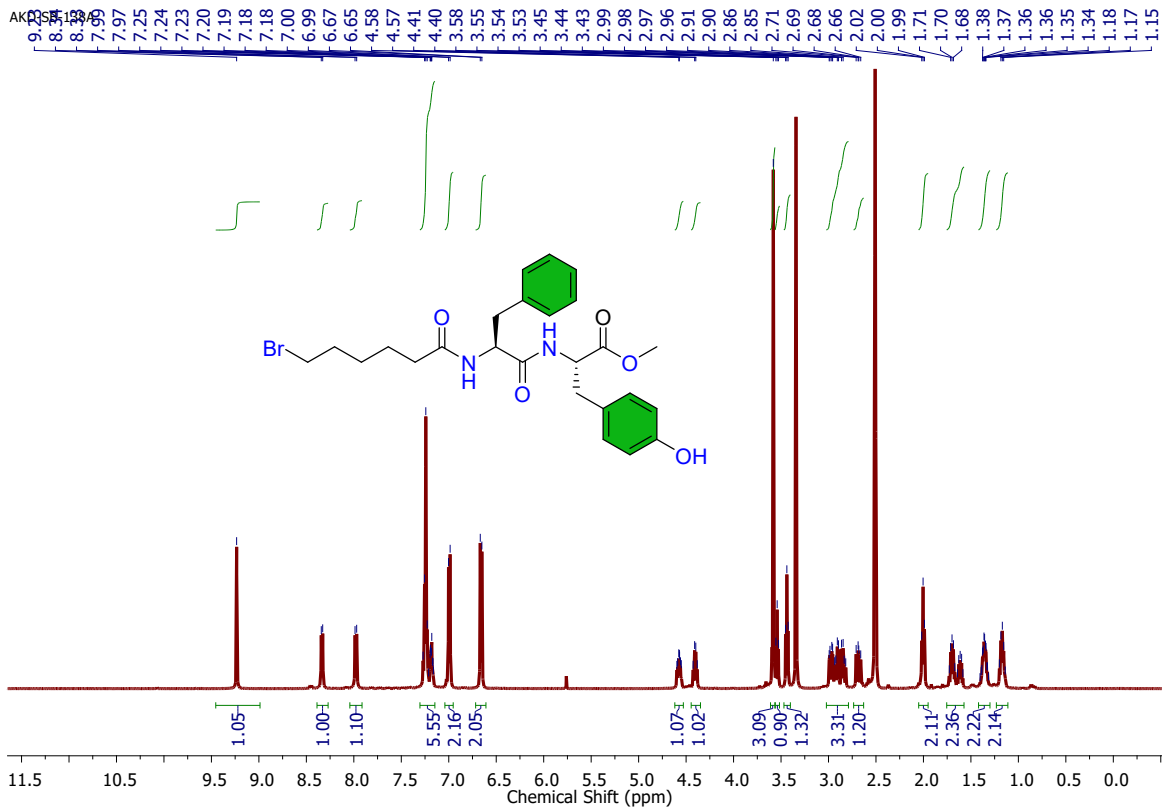


Fig. S16  $^1\text{H}$  NMR (500 MHz,  $\text{DMSO-}d_6$ ) spectrum of **2b**.

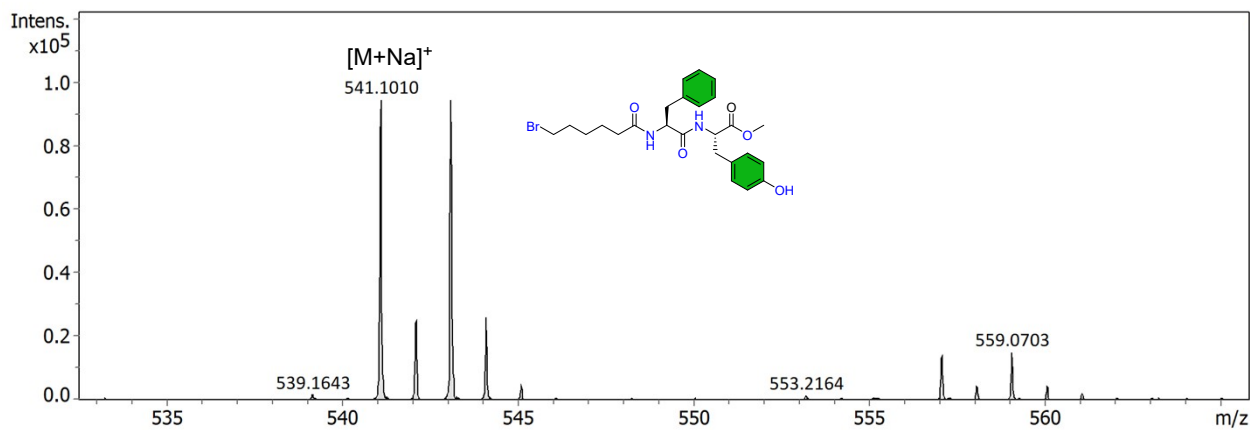


Fig. S17 ESI-MS spectrum of **2b**.

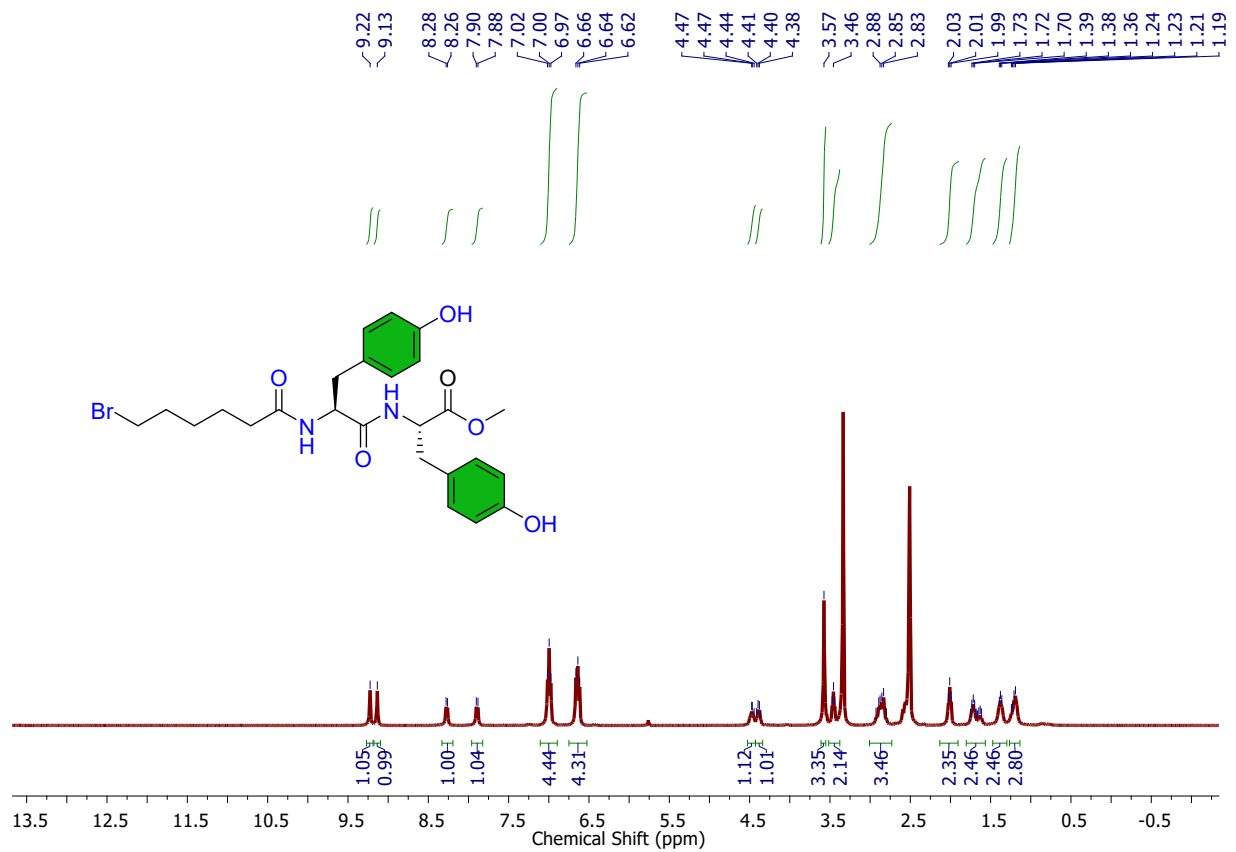


Fig. S18 <sup>1</sup>H NMR (500 MHz, DMSO-*d*<sub>6</sub>) spectrum of **2c**.

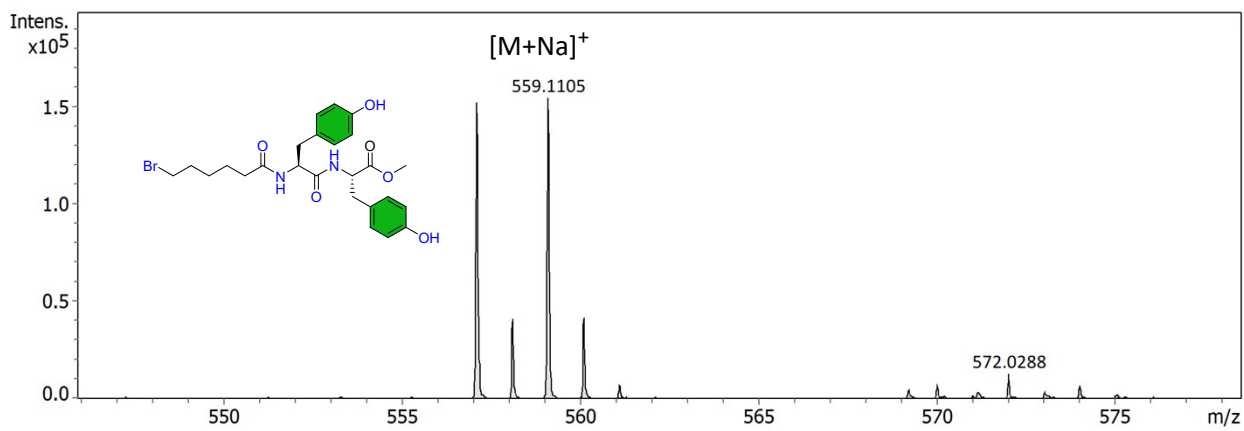


Fig. S19 ESI-MS spectrum of **2c**.

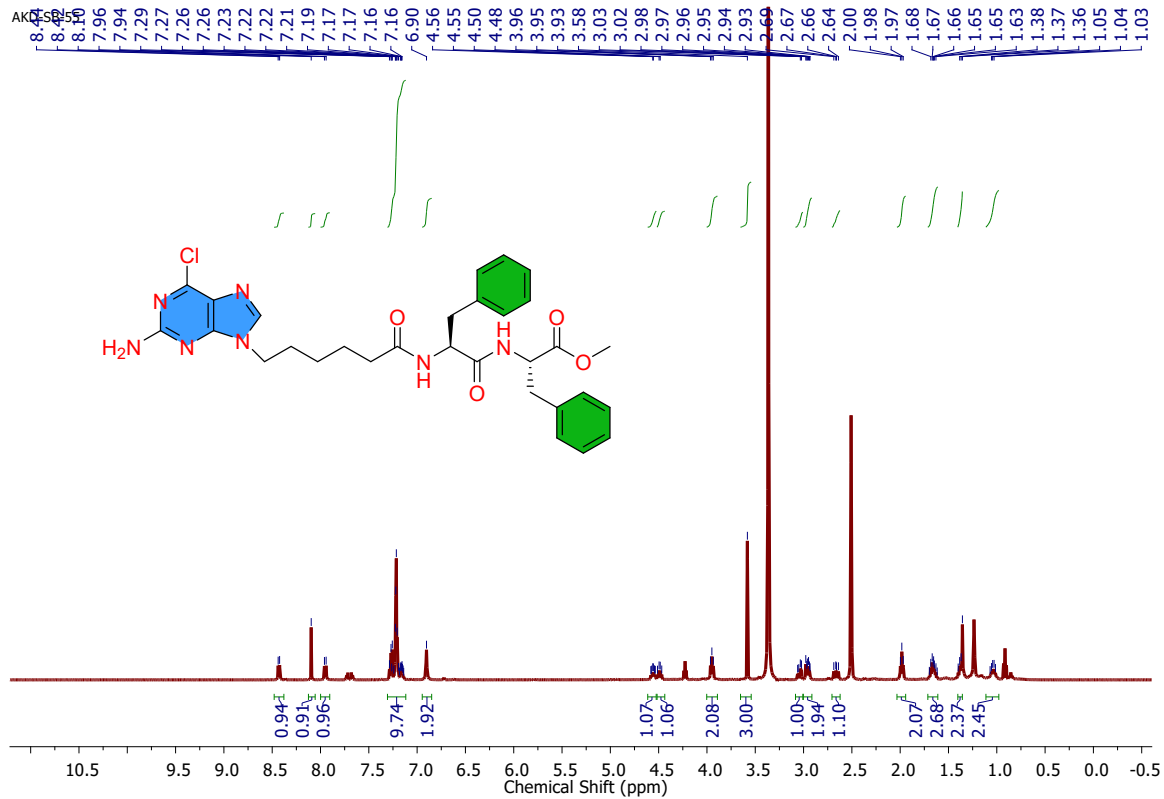


Fig. S20  $^1\text{H}$  NMR (500 MHz,  $\text{DMSO-}d_6$ ) spectrum of **3a**.

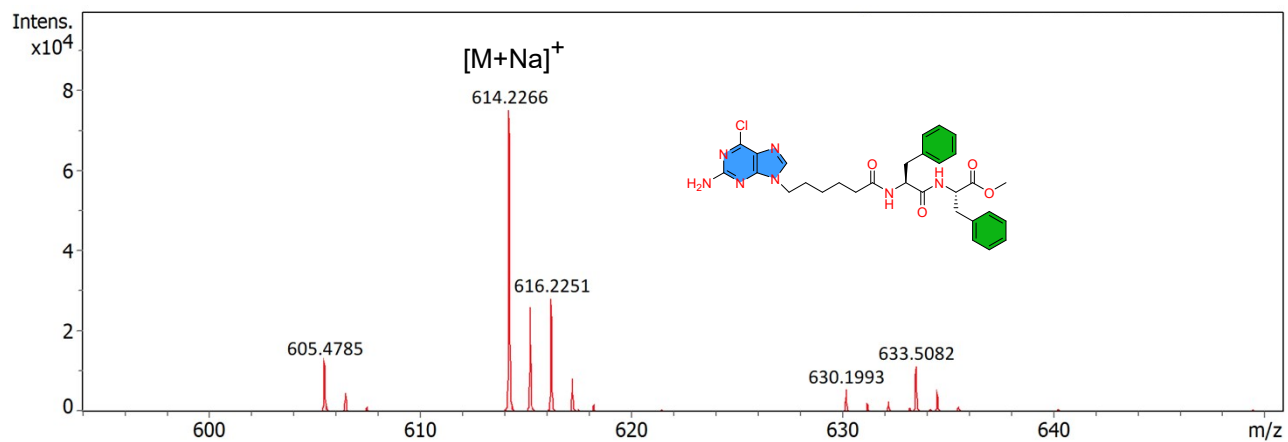


Fig. S21 ESI-MS spectrum of **3a**.

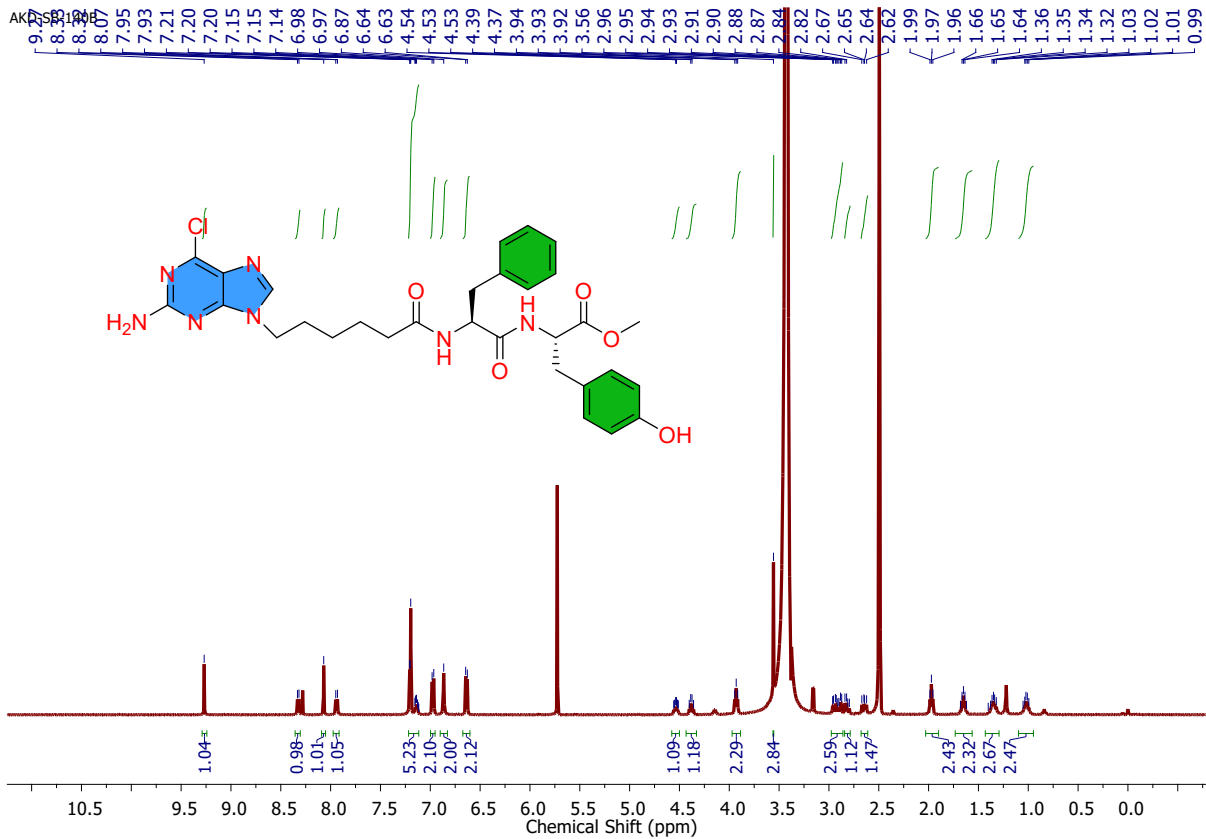


Fig. S22  $^1\text{H}$  NMR (500 MHz,  $\text{DMSO-}d_6$ ) spectrum of **3b**.

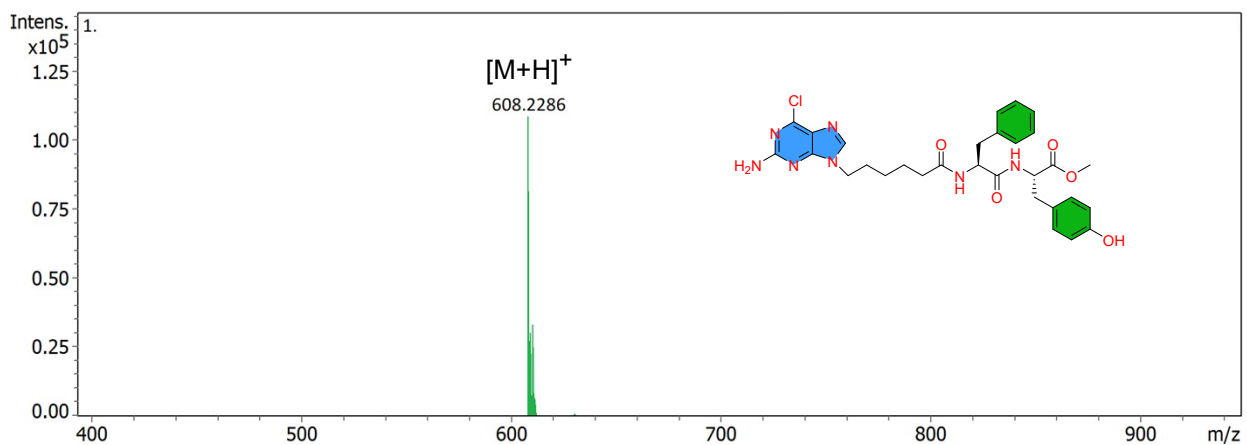
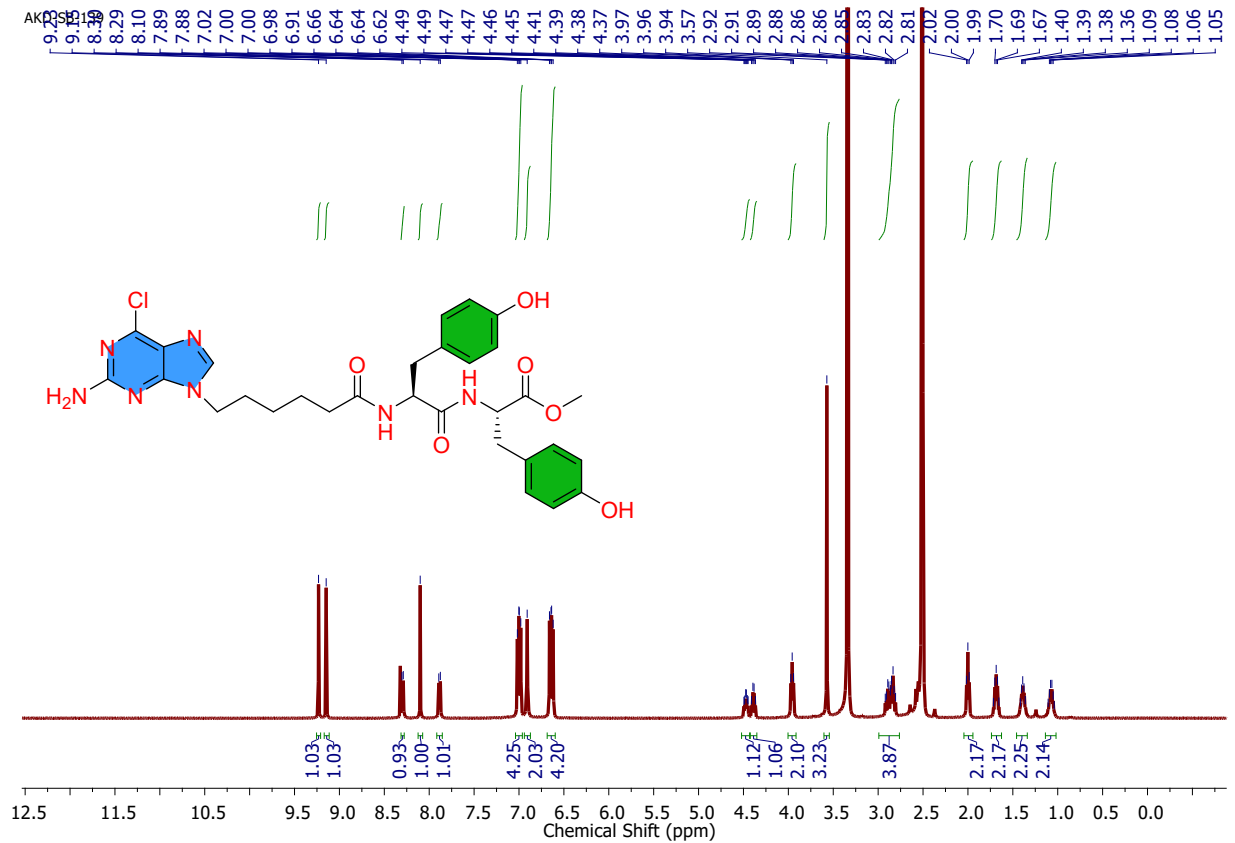
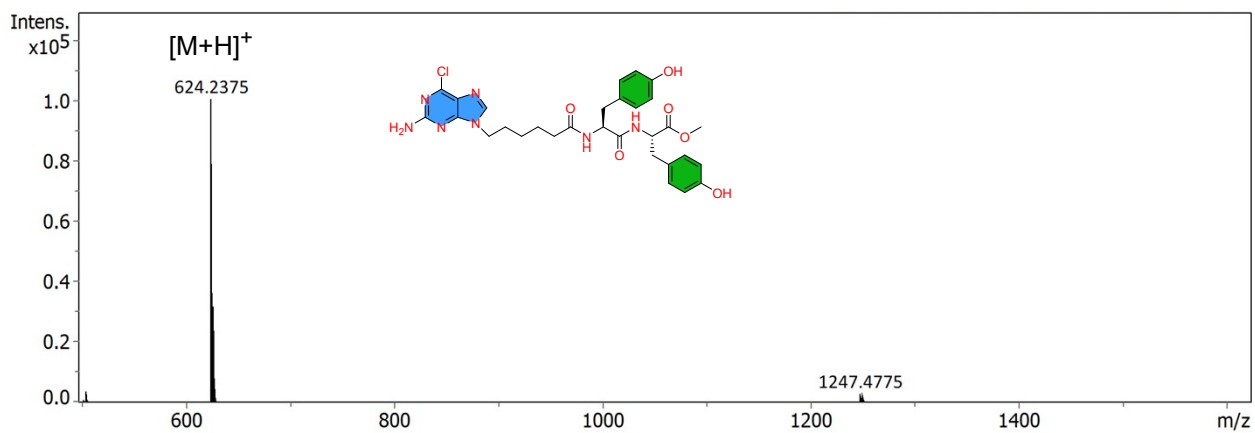


Fig. S23 ESI-MS spectrum of **3b**.



**Fig. S24** <sup>1</sup>H NMR (500 MHz, DMSO-*d*<sub>6</sub>) spectrum of **3c**.



**Fig. S25** ESI-MS spectrum of **3c**.

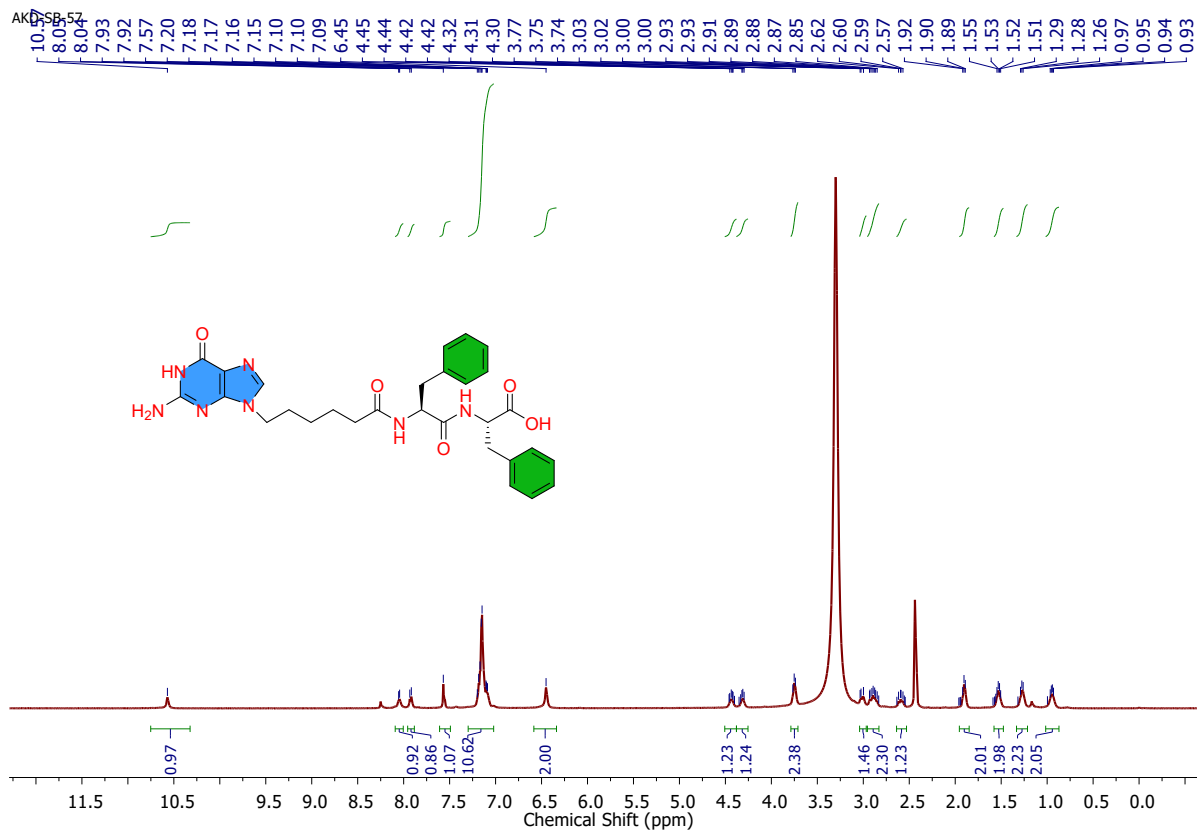


Fig. S26  $^1\text{H}$  NMR (500 MHz,  $\text{DMSO-}d_6$ ) spectrum of NP1.

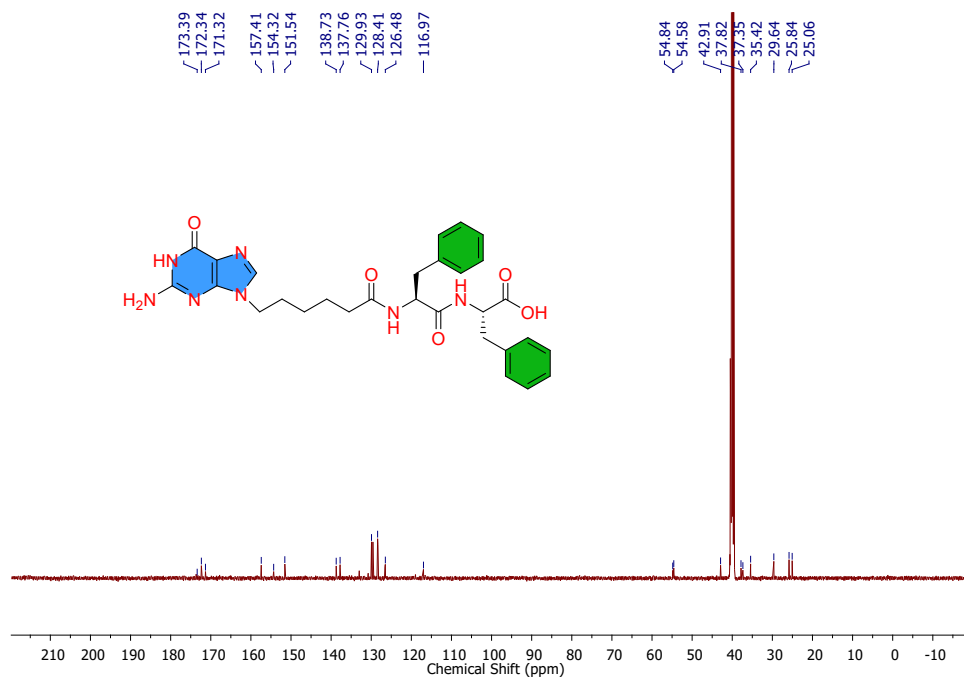


Fig. S27  $^{13}\text{C}$  NMR (125 MHz,  $\text{DMSO-}d_6$ ) spectrum of NP1.

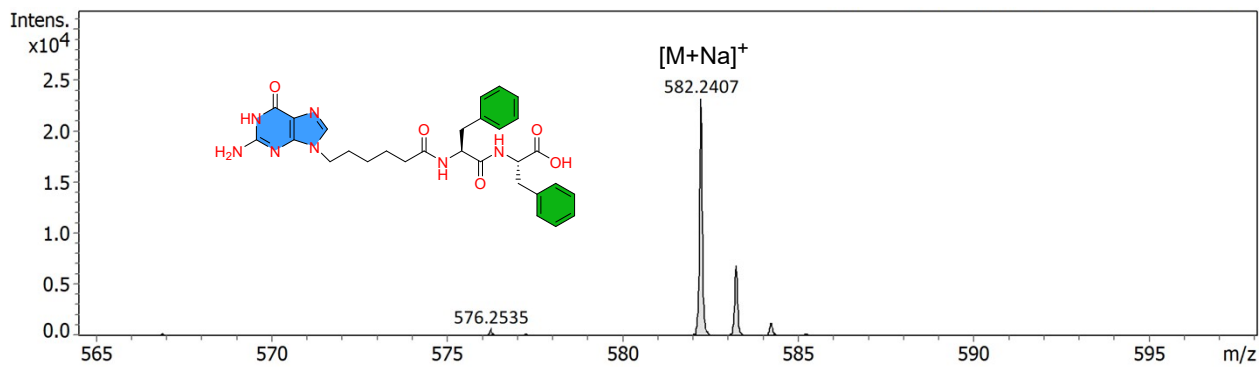


Fig. S28 ESI-MS spectrum of NP1.

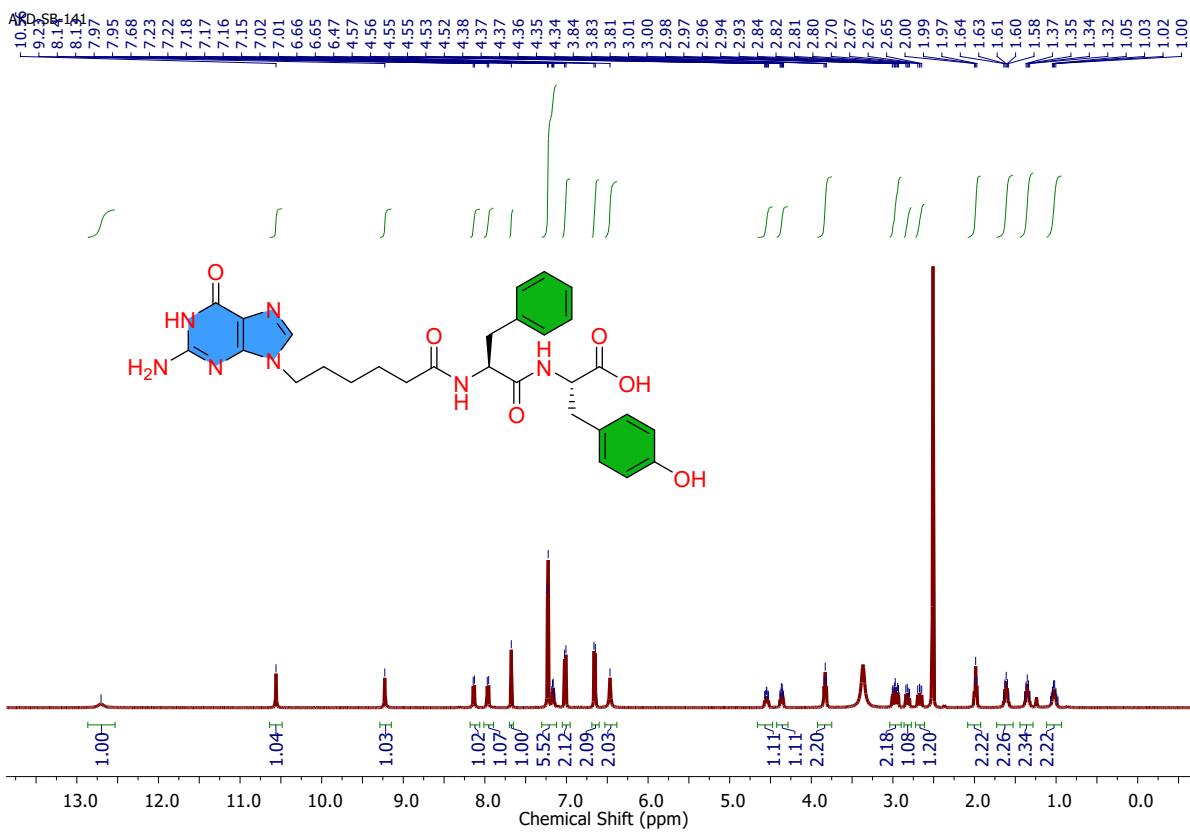
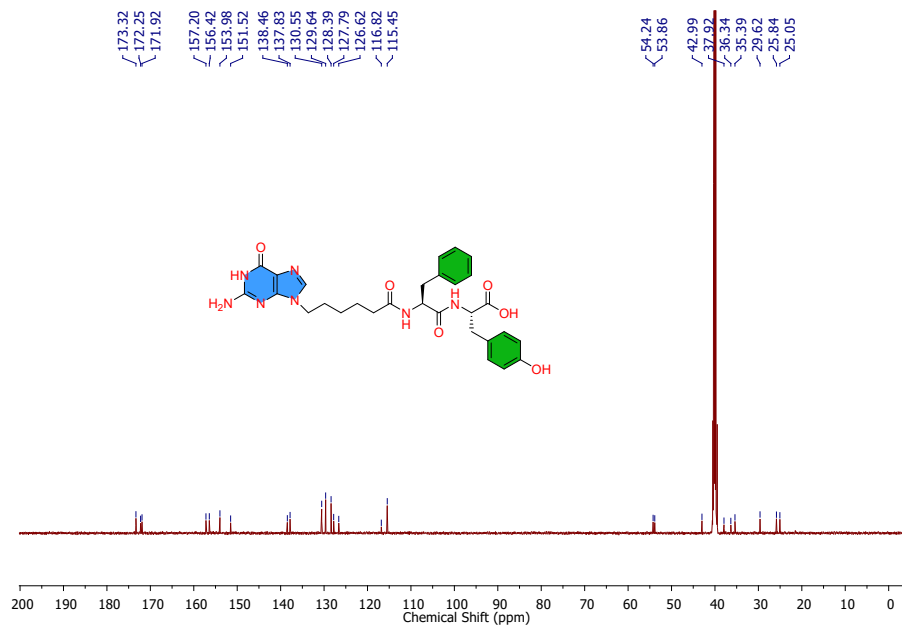
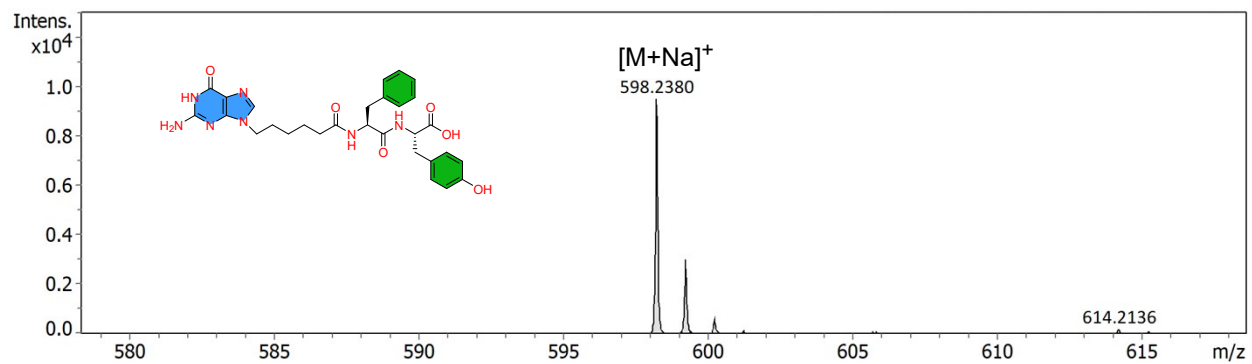


Fig. S29 <sup>1</sup>H NMR (500 MHz, DMSO-*d*<sub>6</sub>) spectrum of NP2.



**Fig. S30**  $^{13}\text{C}$  NMR (125 MHz,  $\text{DMSO-}d_6$ ) spectrum of NP2.



**Fig. S31** ESI-MS spectrum of NP2.

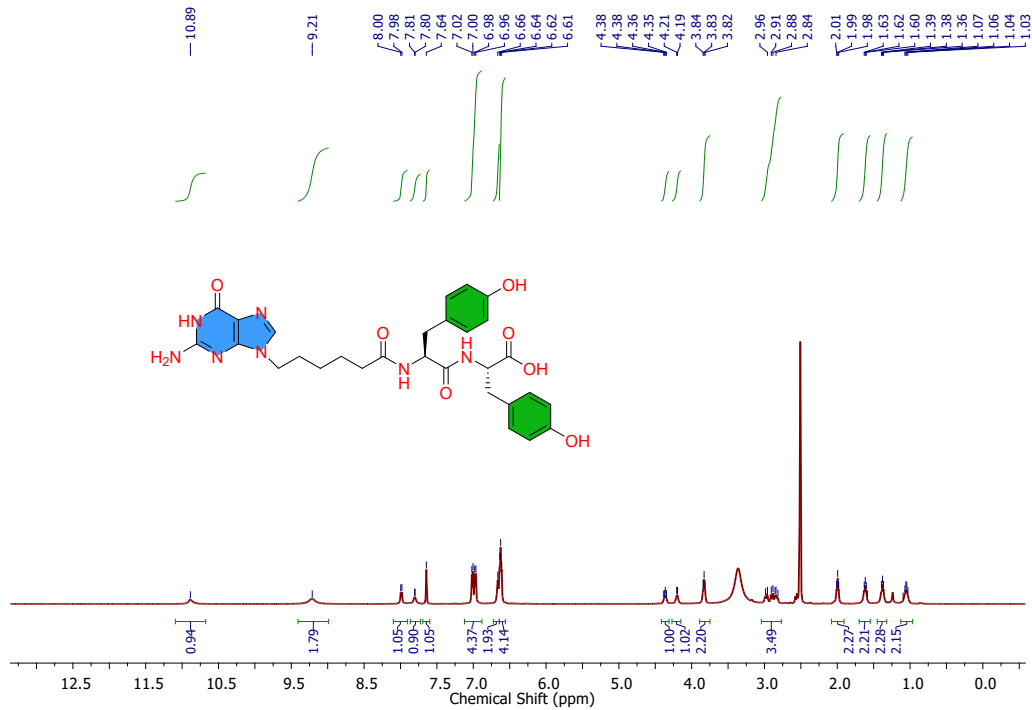


Fig. S32 <sup>1</sup>H NMR (500 MHz, DMSO-*d*<sub>6</sub>) spectrum of NP3.

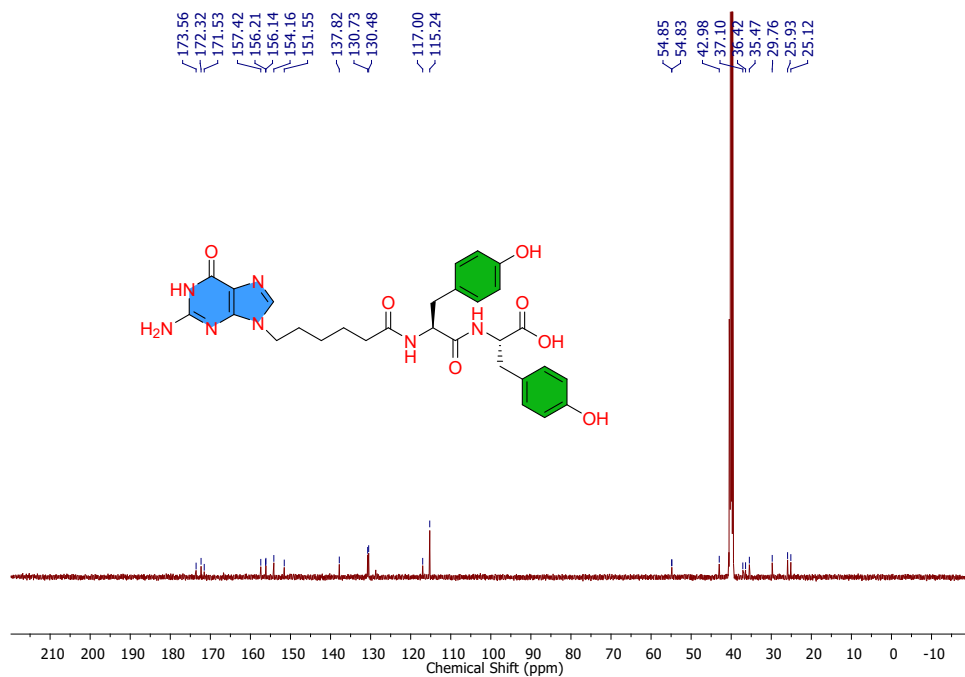
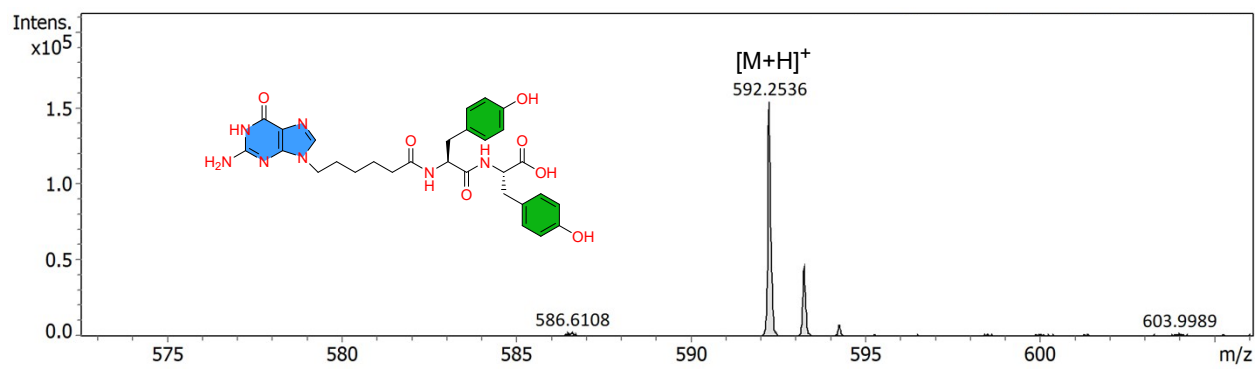


Fig. S33 <sup>13</sup>C NMR (125 MHz, DMSO-*d*<sub>6</sub>) spectrum of NP3.



**Fig. S34** ESI-MS spectrum of NP3.